Immunity & Ageing

RESEARCH

Open Access

Mouse brain contains age-dependent extraparenchymal granular structures and astrocytes, both reactive to natural IgM antibodies, linked to the fissura magna

Clara Romera[1,2,3], Marta Riba[1,2,3], Raquel Alsina[1,2,3], Marina Sartorio[1,2], Jordi Vilaplana[1,2,3], Carme Pelegrí[1,2,3*] and Jaume del Valle[1,2,3*]

Abstract

Background Mouse brains can contain specific polyglucosan aggregates known as Periodic Acid-Schiff (PAS)-granules. Generated in astrocytes, these granules increase with age and exhibit neo-epitopes of carbohydrate nature that are recognized by natural IgM antibodies (IgMs). The existence of neoepitopes on PAS granules suggests the presence of neoepitopes in other brain structures, and this is investigated here. To this end, brain sections from SAMP8 and ICR-CD1 mice were examined at different ages.

Results We have identified two novel structures that, apart from PAS granules, are recognized by natural IgMs. On one side, IgM reactive (IgM^+) granular structures which are placed in the longitudinal fissure, the quadrigeminal cistern, and a region that extends from the quadrigeminal cistern to the interpeduncular cistern. This last region, located between the telencephalon and both the mesencephalon and diencephalon, is designated henceforth as the fissura magna, as it is indeed a fissure and the largest in the brain. As all these regions are extraparenchymal (EP), the IgM^+ granules found in these zones have been named EP granules. These EP granules are mainly associated with fibroblasts and are not stained with PAS. On the other side, some IgM^+ astrocytes have been found in the glia limitans, near the above-mentioned fissures. Remarkably, EP granules are more prevalent at younger ages, while the number of IgM^+ astrocytes increases with age, similarly to the already described evolution of PAS granules.

Conclusions The present work reports the presence of two brain-related structures that, apart from PAS granules, contain neo-epitopes of carbohydrate nature, namely EP granules and IgM^+ astrocytes. We suggest that EP granules, associated to fibroblasts, may be part of a physiological function in brain clearance or brain-CSF immune surveillance, while both PAS granules and IgM^+ astrocytes may be related to the increasing accumulation of harmful materials that occurs with age and linked to brain protective mechanisms. Moreover, the specific localisation of these EP granules and IgM^+ astrocytes suggest the importance of the fissura magna in these brain-related cleaning and immune functions. The overall results reinforce the possible link between the fissura magna and the functioning of the glymphatic system.

*Correspondence:
Carme Pelegrí
carmepelegri@ub.edu
Jaume del Valle
jdelvalle@ub.edu
Full list of author information is available at the end of the article

Keywords Ageing, Brain, Immune surveillance, Natural antibodies, Neo-epitopes, EP granules, Fibroblasts, Astrocytes, Glymphatic system, Fissura magna

Background

The human brain, primarily composed of postmitotic cells, is highly susceptible to the multifaceted effects of ageing [1]. This intricate process involves a cascade of molecular, cellular, and structural changes that impact various aspects of brain function, including learning, memory, and motor performance [2, 3]. Additional alterations, such as a reduction in brain volume and the loss of neurons, dendritic arbor, or synaptic connectivity have been described elsewhere [4, 5]. Moreover, the accumulation of abnormal protein aggregates and polyglucosan structures during ageing and neurodegenerative conditions has also been well-documented [6–9].

In mice, specific age-related polyglucosan aggregates known as PAS granules (due to their positive staining with the Periodic Acid Schiff technique) have been identified in their brain, particularly in the hippocampus. These aggregates have consistently been observed in the brains of several strains of mice, including C57BL/6 [10–12], ICR-CD1 [13, 14], AKR [15], and senescence-accelerated mouse prone mouse 8 (SAMP8) mice [10, 13, 16, 17] among others. The presence of these granules increases with age, becoming more prominent in the brains of aged mice suggesting potential relevance to age-related processes [15, 18]. Remarkably, no granules are evident in the early stages of life. At 3 months of age, only some scattered PAS granules appear in the hippocampus of ICR-CD1 mice, and from 6 months onwards, ICR-CD1 mice show clusters of granules in their hippocampus. In SAMP8 mice, the number of granules is increased respect to the age-matched ICR-CD1 mice, and clustered granules in their hippocampus appear as early as at 3 months of age [13]. Other strains also exhibit a similar pattern of increased PAS granules with ageing [18]. The entorhinal cortex and the piriform cortex exhibit a delayed appearance of granules respect to the hippocampus, indicating a direct correlation with age, albeit with a later onset compared to the hippocampus. Other brain regions such as the olfactory bulb, the cerebellum and the trapezoid body have also been reported to show these granules in aged mice of different strains [18].

These PAS granules exhibit a distinctive round-to-ovoid morphology, they measure 1–3 µm and tend to appear in clusters of 40 to 50 granules. Typically, each cluster is associated with a single astrocyte [19]. In addition to their polyglucosan content, these granules also contain specific proteins, such as glycogen synthase (GS) and p62. GS plays a crucial role in the formation of their polyglucosan content, while p62 is involved in the recollection of residual or deleterious products [20]. While the precise mechanism of granule formation remains a subject of debate, certain ultrastructural studies suggest that astrocytes phagocytose degenerative or deleterious substances and incorporate them into the polyglucosan structure [17, 19].

Consistently, PAS granules exhibit some kind of epitopes of carbohydrate nature which are considered neo-epitopes (meaning newly formed epitopes) since they arise during the granule formation. Commonly, neo-epitopes are targeted by immune surveillance, and are recurrently recognized by natural IgM antibodies present in the plasma [21]. Natural IgMs, which have been evolutionarily fixed and thus are generally interspecific, emerge from innate immunity and are inherently present before birth without external antigenic exposure. These antibodies function as a first line of defense against different pathogens, but also exert a critical role on the maintenance of tissue homeostasis recognizing post-transcriptional modifications of proteins, lipids, and carbohydrate residues to facilitate the elimination of potentially deleterious or residual cellular byproducts [21, 22]. Nevertheless, plasma IgM antibodies cannot cross the blood–brain barrier and thus, in vivo, are incapable of binding the neo-epitopes contained in the PAS granules of mouse brain. In addition, as these PAS granules are intra-astrocytic structures, surrounded by a plasma membrane [19], they do not activate microglia and they remain silent without inducing brain inflammation or interfering with normal functioning of neighboring cells. Thus, PAS granules might be considered structures that accumulate and isolate residual products in order to avoid deleterious processes and brain inflammation or damage.

The presence of neo-epitopes in PAS granules suggests the possibility that neo-epitopes may also be generated or emerge in other structures or regions of the brain, potentially associated with ageing. Thus, the primary objective of the present work is to identify whether neo-epitopes like those described in PAS granules exist in other brain regions. Secondarily, this study aims to determine if their occurrence correlates with ageing.

Hence, in this work we will determine the presence of additional structures detectable by natural IgMs in other mouse brain regions beyond those previously described. Subsequently, we will determine if, in these

structures, the neo-epitopes recognized by IgMs have a glycosidic nature. Moreover, we will investigate whether the newly detected structures contain polyglucosan as PAS granules do and thus exhibit positivity to PAS staining, and we will study if they contain p62 protein (as also PAS granules do). Additionally, we will explore their association with astrocytes and evaluate any similarities with PAS granules in this regard. Finally, we will examine the potential relationship between the newly identified structures and ageing.

Methods

Animals and brain processing

Male SAMP8 and ICR-CD1 mice aged 3, 6 and 12 months were studied. 7 animals of each age and strain were used. They were kept in standard conditions of temperature (22 ± 2° C) and 12-h light–dark cycles (300 lx/0 lx). Throughout the study, they had access to food and water ad libitum. The day of the tissue harvest, animals were weighed, and the results were noted. Animals were then anesthetized with 80 mg/kg of sodium pentobarbital by an intraperitoneal injection. Then, to obtain the brain, the thoracic cavity was opened and the animals received an intracardiac gravity-dependent perfusion of 50 ml of phosphate-buffered saline (PBS, pH 7.2). After the perfusion, brains were dissected, frozen by immersion in isopentane chilled in dry ice, and stored at – 80° C until sectioning. Thereafter, frozen brains were embedded in OCT cryostat-embedding compound (Tissue-Tek, Torrance, Calif., USA). Coronal sections of 20 µm-thick were cut on a cryostat (Leica Microsystems, Germany), placed on slides and stored at -20° C until further use.

Immunohystochemistry

Brain sections were defrosted for 10 min at room temperature and a hydrophobic marker was used to draw an isolating well around each brain slice. Sections were rehydrated with PBS for 5 min and after that, sections were blocked and permeabilized for 20 min with blocking buffer-triton (BB) made of 1% bovine serum albumin (BSA, A3059- 50G, Sigma-Aldrich) and 0.1% Triton X-100 (T8532-100ML, Sigma-Aldrich), diluted in PBS. Slides were washed with PBS twice and incubated overnight at 4 ºC with the corresponding primary antibodies: IgMs from human serum (1/25, I8260, Merck), chicken monoclonal IgY anti-GFAP (glial fibrillary acidic protein, 1/300, AB5541, Merck), rabbit monoclonal anti-p62 (1/50, AB5541, Abcam), rabbit monoclonal Glycogen Synthase (1/100, 3886S, Cell Signaling Techonologies), rabbit monoclonal IgG anti-vimentin (1/200, ab254015, Abcam) and biotin mouse monoclonal IgG2a Cytokeratin 5/8 Antibody (C-50) (1/200, NBP2- 47824B, Bio-techne), all of them diluted in BB.

The following day, the sections were washed twice with PBS and the corresponding secondary antibodies and fluorescent reagents were used: Alexa Fluor (AF) 488 goat anti-human IgM (A21215, Life Technologies), AF594 goat anti-human IgM (A21216, Life Technologies), AF488 goat α-chicken IgY (A11039, Invitrogen), AF647 goat α-chicken IgY (A21449, Invitrogen), AF488 donkey α-rabbit IgG (21,206, Invitrogen), AF555 donkey α-rabbit IgG (A-31572, Invitrogen), AF647 donkey α-rbb IgG (A-31573, Invitrogen) and AF488 streptavidin (S32354, Invitrogen), all of them diluted at 1/250 in BB. The secondary antibodies were filtered with a Millex®-GV 0.22 µm filter (Merck Millipore Ltd.) to reduce the possibility of artifacts and added to the sections for incubation 1 h at room temperature. Additionally, Hoechst stain 33258 (Fluka) was incorporated at 2 µg/mL in the last 5 min of the secondary antibodies incubation to stain the nuclei of the cells. Finally, slides were washed and coverslipped with Fluoromount (Electron Microscopy Sciences, Hatfield, PA, USA). Staining controls were performed by incubating brain sections with BB instead of the primary antibody.

PAS staining

In order to determine the presence of PAS-positive structures in the different brain regions, a PAS staining was performed. Before starting the staining, the samples were defrosted at room temperature and fixed with Carnoy's solution (60% ethanol, 30% chloroform, and 10% glacial acetic acid) for 10 min. After the fixation, slices were washed 10 times in distilled water and immersed in periodic acid (0.25%) for 10 min (19324–50, Electron Microscopy Sciences). A second washing with distilled water for 3 min was carried out. Secondly, the samples were immersed in Schiff's reagent (26052–06, Electron Microscopy) in staining jars tightly closed and protected from light. After 10 min, slices were washed with distilled water for 5 min or until pinkish coloration was reached. Finally, 3 consecutive washes were performed with distilled water and the samples were dehydrated in alcohols of 70%, 90%, 100%, and xylene (XI00502500, Scharlau) twice for 10 min. The different alcohols used were prepared with ethanol absolute (ET00051000, Scharlau) and H_2Od. Slices were cover-slipped with Eukitt mounting medium (Eukitt, Fluka Analytical).

Sugar preabsorption studies

In order to know if IgM positive (IgM^+) structures, i.e. structures that become stained with human IgMs, contain neo-epitopes of carbohydrate nature, the IgM primary antibodies were preadsorbed with a mixture of the monosaccharides as before [23]. The mixture of monosaccharides contains D-Glucose (Scharlab, GL01271000),

D-(+)-Mannose (Sigma Aldrich, M2D69), D-(+)-Galactose (Sigma Aldrich, G0750), N-AcetylGalactosamine (Sigma Aldrich, A2795) and D-(-)-Fructose (Sigma Aldrich, F0127). Three different solutions were prepared at 0 (control), 0.2 M and 0.4 M of each sugar in PBS and the mixtures were maintained overnight at 4 °C with agitation. Then, brain sections were incubated with the mixture instead of the primary antibody and the immunofluorescence protocol was followed afterwards as detailed above.

Gamma-amylase pre-treatment

For the pre-treatment of the brain samples with γ-amylase (A7420, Merck), a solution of γ-amylase was prepared by dissolving 10 mg in 2 mL of acetate buffer (pH 4.8, 0.016 M) to reach a concentration of 200 U/mL. After agitation until complete dissolution, a 100 U/mL solution was prepared by diluting 1 mL of the initial solution with an equal volume of acetate buffer. Enzyme and acetate solutions were pre-heated in the water bath at 45 °C. Tissue sections were rehydrated in PBS for 5 min and then covered with 40 µL of digestion solution (0 U/mL (control), 100 U/mL and 200 U/mL) for 22 h at 45 °C. After the incubation, brain samples were washed three times with PBS for 5 min each to remove the excess of enzyme solution and the immunofluorescence protocol was followed in the same manner as above.

Image acquisition

Imaging was conducted with a fluorescence microscope (BX41, Olympus, Germany) using excitation wavelengths of 360–370 nm, 470–495 nm, 540–550 nm, and 590–650 nm and detecting emission wavelengths of 420–460 nm, 510–550 nm, 575–625 nm, and 663–737 nm, respectively. The subsequent merging of the different channels was performed using Image J software (National Institute of Health, USA). Image enhancement to optimize visualization of the different stainings was also performed with ImageJ programme, ensuring uniform treatment across different strains and age groups for each single staining.

Quantification of IgM positive structures and PAS granules

As it will be described in the results, we detected some extraparenchymal (EP) IgM^+ granules different from the previously described hippocampal PAS granules, and some astrocytes that were IgM^+.

To quantify the EP granules, a coronal brain section of each animal (between bregma -1,91 and bregma -2,79 mm, according to Paxinos and Franklin's mouse brain atlas [24]) was stained with IgMs and examined with the microscope (BX41, Olympus, Germany). In each section, and for each region of interest (regions 1 to 8, described in results), three blinded observers quantified the amount of granules using a subjective score ranging from 0 (denoting absence of granules) to 3 (representing maximum presence of granules). PAS granules present in the hippocampus of each section were also quantified by the same three blinded observers, who assigned a subjective score ranging from 0 (denoting absence of granules in the hippocampus) to 5 (representing maximum presence of granules in the hippocampus). Furthermore, a similar rating system was used to score the amount of IgM^+ astrocytes, with scores from 0 (indicating absence of IgM^+ astrocytes) to 3 (reflecting maximum presence of IgM^+ astrocytes). The mean of the scores obtained by the three observers in each quantification and region was used for analysis.

Statistical analysis

Studies of correlation between variables were performed using the Correlation module of SPSS Statistics (IBM). The ANOVA module of SPSS Statistics has been used in order to analyse the effect of the factors strain (SAMP8 or ICR-CD1) and age (3, 6 and 12 months) on different dependent variables (body weight, amount of PAS granules, amount of EP granules in the different regions of interest, and number of astrocytes IgM^+). Post hoc comparisons were performed with the Tukey test and differences were considered significant when $p < 0.05$. Even so, this study not only considered p values but also integrated them with other findings to reach conclusions based on a general view. As remarked in the Editorial of Nature dated 20th March 2019 [25], relying solely on p values for determining significance may result in biased analyses, exaggerated false positives, and overlooked genuine effects. Therefore, it's crucial to incorporate logic, background knowledge, and experimental design with p values when drawing conclusions and assessing their reliability.

Results

Presence of extraparenchymal IgM^+ granular structures

A first screening of coronal sections obtained from ICR-CD1 and SAMP8 mice aged 3, 6 and 12 months immunostained with IgM permitted to observe the presence of some extraparenchymal (EP) IgM^+ granular structures, designated as EP granules, that are different to the previously described PAS granules in terms of localization and clustering. These granules were located in the specific brain regions that are detailed in Fig. 1A. As shown in the figure, granules were placed along the longitudinal fissure (between the two brain hemispheres), the quadrigeminal cistern, and a region comprised between the telencephalon and the diencephalon, that will be designated henceforth as the fissura magna as it is indeed a fissure and the

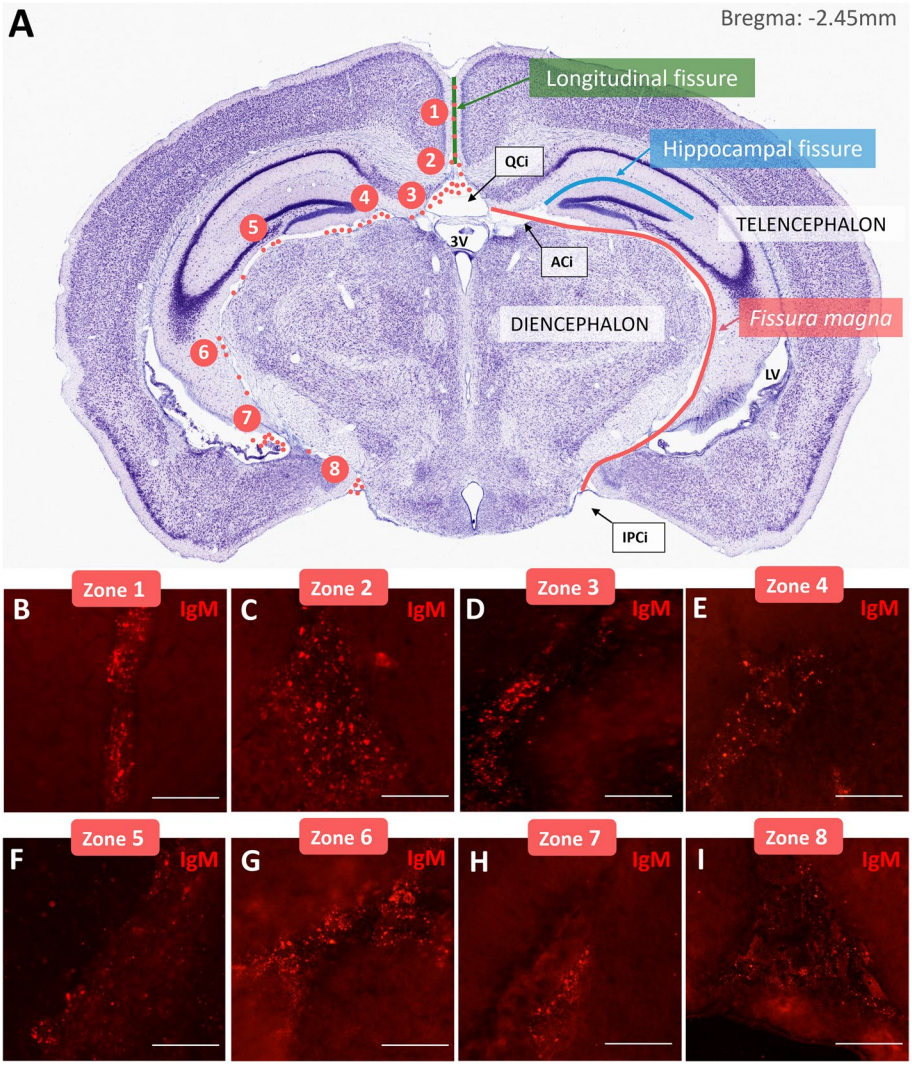

Fig. 1 Presence of EP granules in mouse brain. **A** Nissl stained coronal section of a mouse brain at bregma -2,45 mm showing EP granules localization. Granules (red dots) are indicated only in the right hemisphere whereas the left hemisphere is used to indicate the name of the different structures. As can be observed, granules were placed along the longitudinal fissure (green line), the quadrigeminal cistern (QCi), and the fissura magna (red line) and concentrated in specific regions numbered from zone 1 to zone 8. **B-I** Representative images of EP granules in each described region in a representative 3-month-old SAMP8 mouse. (ACi) ambient cistern, (IPCi) interpeduncular cistern. Figure 1A is adapted from [26]. Scale bars: 50 µm

largest one in the brain. Note that for bregma lower than -3 mm, this fissure continues between the telencephalon and the mesencephalon.

Although EP granules were placed all along these fissures, they usually concentrated in specific regions numbered from 1 to 8 in the Fig. 1A. The region 1 is located in the longitudinal fissure. The region 2 is located in the upper part of the quadrigeminal cistern. The region 3 is located in the contact between the quadrigeminal cistern and the fissura magna. The region 4 is placed where the hippocampal fissure arises from the fissura magna. The region 5 is located in the lateral region of contact between the fissura magna and the dentate gyrus. In the region 6, the fissura magna begins to contact with the fimbria. In the region 7, the fissura magna is adjacent to the root of the choroid plexus of the lower horn of the lateral ventricle. Finally, the region 8 is located at the inferior part of the fissura magna, near the interpeduncular cistern (Fig. 1 B-I).

Characterization of EP granules

In contrast with PAS granules, that are typically observed forming clusters in the hippocampus each associated with an astrocyte (Fig. 2E), the EP granules reported here

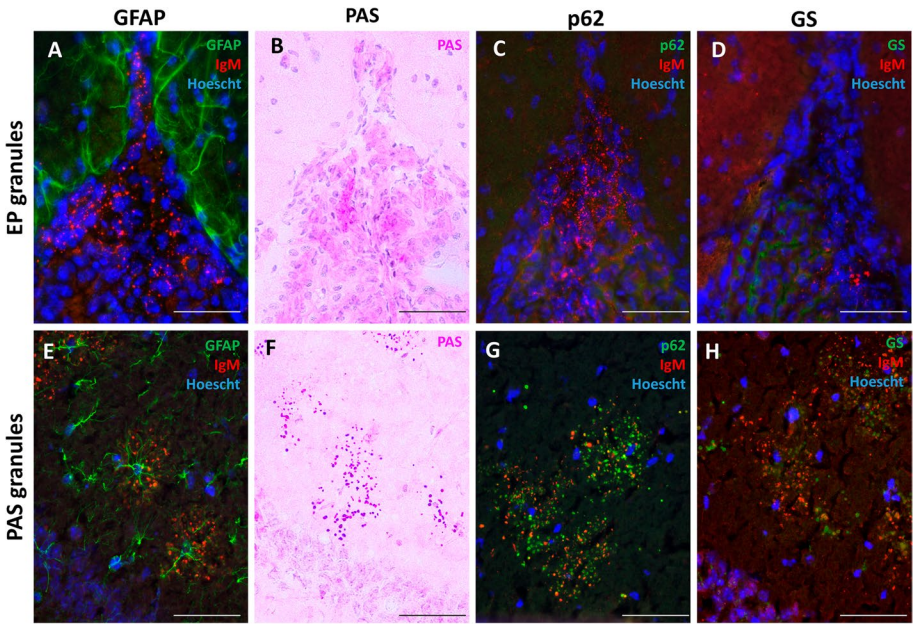

Fig. 2 Characterization of EP granular structures in mouse brain. When sections were stained with IgM to label the EP granules and with GFAP to stain astrocytes, we observed that EP granules from the fissures showed no relation with astrocytes (**A**), while the clusters of hippocampal PAS granules were found in areas occupied by astrocytes (**E**). When staining the sections with PAS, the EP granules were not stained (**B**), unlike PAS granules, which, as expected, were stained with the PAS stain (**F**). EP granules were not stained with p62 or GS (**C** and **D**, respectively), while PAS granules of the hippocampus were positive to these stainings (**G** and **H**, respectively). Sections **A**, **C**, **D**, **E**, **G** and **H** were also stained with Hoechst (cell nuclei, blue). Scale bars: 50 µm

exhibited a dispersed distribution and lack association with astrocytes (Fig. 2A).

We conducted a PAS stain on brain slides as this method is commonly employed to identify hippocampal PAS granules. Our findings revealed that the EP granules did not exhibit these positive staining (Fig. 2B) while PAS granules in the hippocampus did (Fig. 2F). In fact, this staining defines the named PAS granules. Given the established association of the p62 protein with hippocampal PAS granules [20], we specifically investigated the presence of p62 within the EP granules found in the longitudinal fissure, the quadrigeminal cistern and the fissura magna. Immunofluorescence analysis revealed the absence of p62 within these granules (Fig. 2C), another distinction from hippocampal PAS granules, which are associated to p62 labelling (Fig. 2G). Finally, staining to detect GS also failed to reveal the presence of this protein in the EP granules (Fig. 2D) while, as described in the literature [20], it could be seen in hippocampal PAS granules (Fig. 2H).

On the other hand, considering that these granules in the fissures are recognized by IgMs, which can bind to neoepitopes, and acknowledging the glucidic nature of the neo-epitopes within PAS granules, we conducted experiments to explore whether these IgM antibodies recognize carbohydrate epitopes within EP granules (Fig. 3A-D). Preadsorption of IgM antibodies was carried out with various carbohydrates at increasing concentrations from 0 to 0.4 M. Figure 3 shows that IgM staining reveals EP granules in the fissures when the primary antibody was not preadsorbed with sugars (Fig. 3A) and the staining disappeared when sugars were added at a concentration of 0.4 M (Fig. 3B). PAS granules exhibited comparable behavior, with positive staining observed when the primary IgM antibody was not preadsorbed with sugars (Fig. 3C) and a loss of staining when sugars were added (Fig. 3D). Supplementary Fig. 1 (A-F) illustrates that the staining of these structures gradually diminishes as the sugar concentration increases.

To characterize the glucidic composition of the EP granules, brain sections were incubated with γ-amylase. EP granules in the fissures seemed resistant to this digestion, and several of them could still be observed after the highest γ-amylase concentration (Fig. 3E and F). However, incubation with γ-amylase resulted in the elimination of IgM staining in the PAS granules of the hippocampus (Fig. 3G and H). Indeed, amylase digestions at lower concentrations had almost no impact on IgM staining of EP granules (Suppl. Figure 1 G-I), while hippocampal PAS granules were affected by all concentrations of γ-amylase (Suppl. Figure 1 J-L).

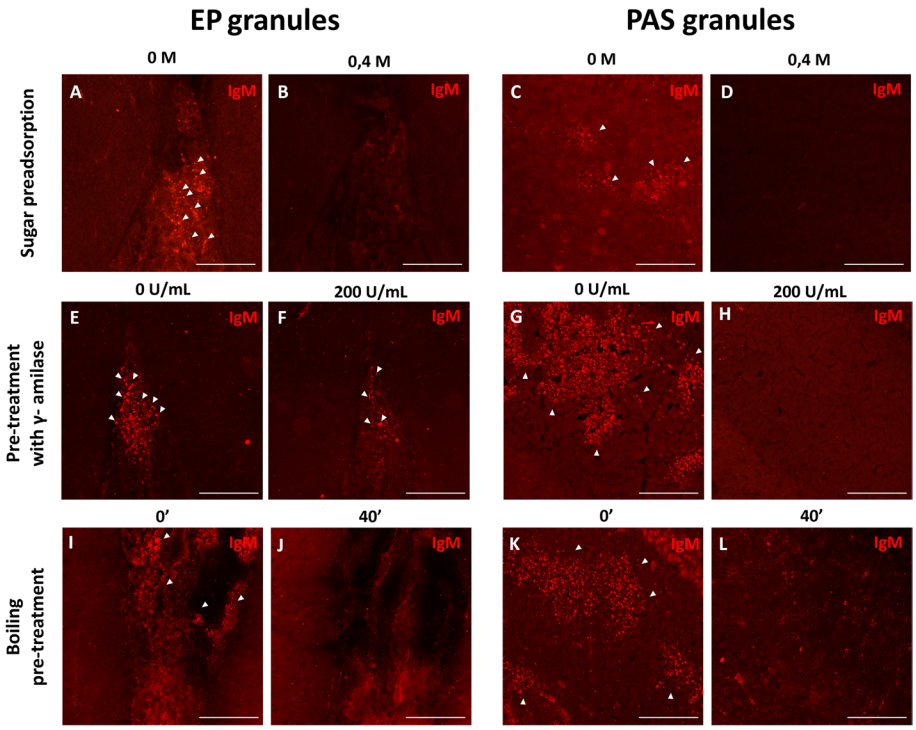

Fig. 3 Carbohydrate characteristics of EP granules vs PAS granules. **A**-**D** Effect of the preadsorption of IgM antibodies with a 0.4 M sugar mixture in the IgM staining (red) of EP granules from the fissures (zone 2, A and B) and in PAS granules from the hippocampus (C and D). **E–H** Effect of the pre-treatment with 200 U/mL of γ-amylase on the staining with IgM in EP granules (zone 2, E and F) and in PAS granules from the hippocampus (G and H). **I**-**L** Effect of a 40 min boiling pre-treatment on the staining with IgM in EP granules (zone 2, I and J) and in PAS granules from the hippocampus (**K** and **L**). Scale bars: 100 µm

Furthermore, considering the common practice of boiling for antigen retrieval, we immunostained brain sections with IgM after boiling them at 100ºC for 40 min. Remarkably, after the 40-min boiling in citrate, the IgM staining of the EP granules in the fissures disappeared (Fig. 3I and J), as also happened with PAS granules of the hippocampus (Fig. 3K and L).

Cell populations associated to EP granules

Given the high presence of cell nuclei in the areas of the longitudinal fissure, the quadrigeminal cistern and the fissura magna where EP granules were detected, we conducted a series of immunohistochemical staining to elucidate the cell populations associated with these granules.

Firstly, brain sections were triple-immunostained for IgM, GFAP, and vimentin (Fig. 4A). IgM permitted to observe the EP granules, GFAP was used to stain the astrocytes and the glia limitans (which are GFAP positive and vimentin positive), and vimentin to stain fibroblasts (which are vimentin positive and GFAP negative) and also astrocytes. The vast majority of cells harbouring EP granules exhibited vimentin positivity but lacked GFAP expression, indicating that these cells are fibroblast and not astrocytes. Moreover, given that the astrocytes in the glia limitans separate the brain parenchyma from the pia mater and the subarachnoidal space, and because of dura and arachnoid maters do not penetrate to the fissures, these fibroblasts must be sited in the pia mater. Consistently, a layer of pial fibroblasts separates the pia and the glia limitans [27]. Therefore, we can deduce that these granules reside outside the brain parenchyma and are in contact with cells that have a fibroblastic rather than an astrocytic identity. Moreover, a few EP granules were also found in the root of the choroid plexus. To further explore these few granules, we stained additional brain sections with IgM, anti-cytokeratin (to stain choroid plexus epithelial cells) and with anti-vimentin (for fibroblasts). As can be observed in Fig. 4B, most EP granules were associated with vimentin staining, suggesting also a selective association of these granules with the fibroblasts adjacent to the choroid plexus. Therefore, all these EP granules were found outside the brain parenchyma, in areas such as the pia mater, associated with fibroblasts.

All the results regarding the characterization of these EP granules and the comparison with hippocampal PAS granules are summarized in Table 1.

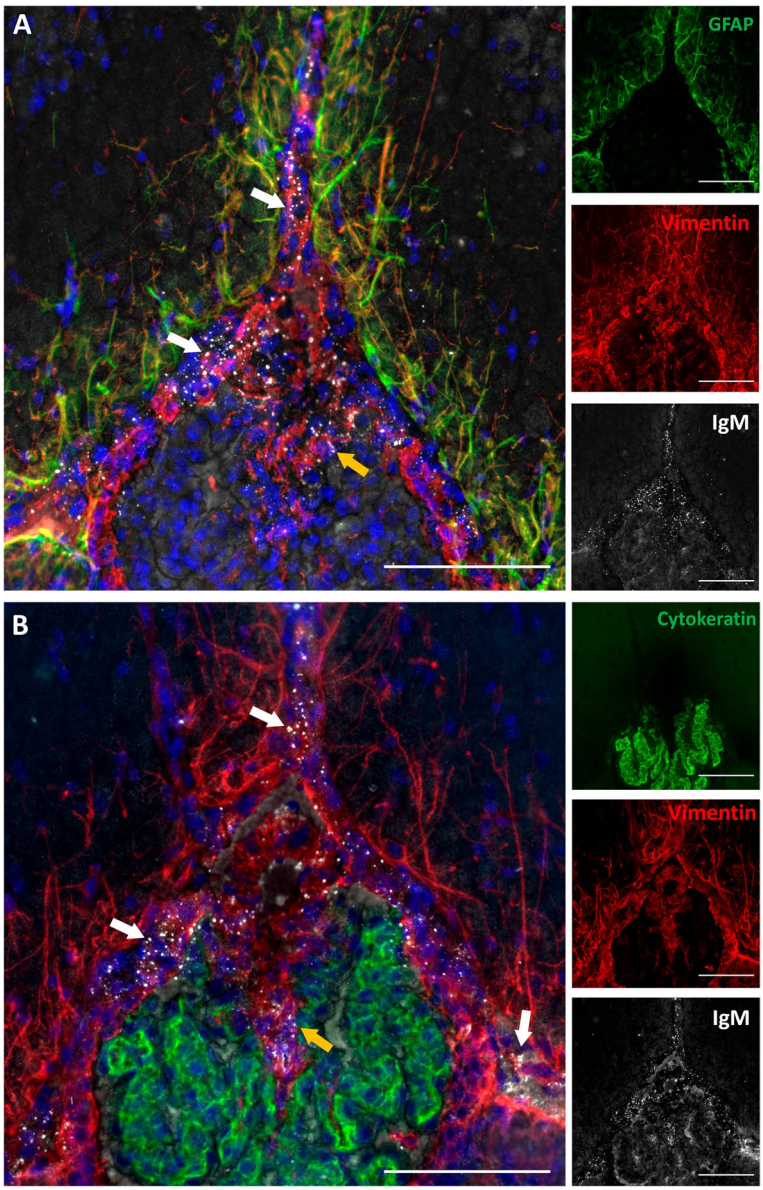

Fig. 4 Cell populations associated to EP granular structures. **A** Representative sections of zone 2 from a 3-month-old SAMP8 mouse immunostained with anti-GFAP (green), anti-vimentin (red), and IgM (white) antibodies, showing merged and separated channels; **B** Representative sections of zone 2 from a 3-month-old SAMP8 mouse immunostained with anti-cytokeratin (green), anti-vimentin (red) and IgM (white) antibodies, showing merged and separated channels (**B**). All sections were stained with Hoechst (cell nuclei, blue). White arrows indicate EP granules in the pia mater; orange arrows indicate EP granules in the root of the choroid plexus. Scale bars: 100 µm

Presence of IgM$^+$ astrocytes

In 12-month-old aged mice from both SAMP8 and ICR-CD1 strains, we noted the presence of astrocyte-like cells exhibiting IgM staining located near the longitudinal fissure, the quadrigeminal cistern and the fissura magna. These astrocyte-like cells IgM$^+$ were scarcely seen in 3- or 6-month-old animals.

Colocalization of IgM staining with GFAP corroborated the astrocytic identity of these cells, proving the presence of neo-epitopes in astrocytes (Fig. 5A). Notably, only the astrocytes closest to the fissures were IgM$^+$ (Fig. 5A1 and 5A2). Although these astrocytes IgM$^+$ were located in regions near the longitudinal fissure, the quadrigeminal cistern and the fissura magna, they were never found associated to the areas where hippocampal PAS granules were found.

As happened with the granules found in the fissures, the preadsorption of the IgM antibodies with sugars

Table 1 Comparison of the characteristics of EP granules and PAS granules

	EP granules	PAS granules
Localization	Longitudinal fissure, quadrigeminal cistern and fissura magna	Hippocampus[a]; piriform cortex, entorhinal cortex, olfactory bulb, cerebellum and trapezoid body
Astrocytic association	-	+
Fibroblast association	+	-
PAS staining	-	+
Presence of p62	-	+
Presence of GS	-	+
Reactive to IgM	+	+
Glucidic neoepitopes	+	+
Sensitivity to γ-amylase	low	high
Sensitivity to boiling treatment	+	+

Granule characteristics are indicated as positive (+) or negative (-)

[a] Predominant region

caused the disappearance of IgM staining on these astrocytes (Fig. 5B), thus indicating that these astrocytes near the fissure exhibited glucidic structures specifically recognized by IgMs. On the other hand, treatment of brain slices with γ-amylase did not affect the IgM positivity of these astrocytes for IgM (Fig. 5C). Finally, exposure of brain samples to boiling for antigen retrieval, following a similar protocol than before, diminished IgM positivity in astrocytes (Fig. 5D).

Body weight analysis

All animals were weighed just before their sacrifice and obtained values are shown in Fig. 6A. The statistical analysis performed by ANOVA, defining both the strain and the age at sacrifice as independent variables and including in the model the interaction between them, indicated that both variables and their interaction have a significant effect on the weight of the animals ($p < 0.01$ for strain, $p < 0.05$ for age and $p < 0.05$ for the interaction). This interaction indicates that age impacts the two strains differently. As illustrated in Fig. 6A and consistent with the characteristics of each strain [28, 29], post hoc comparisons indicate that the mean body weight of ICR-CD1 mice was higher than that of the SAMP8 animals at each time point. Moreover, the body weight of ICR-CD1 mice progressively increased from 3 to 12 months, with 12-month-old animals weighing more than their younger littermates. In contrast, SAMP8 mice exhibited an increase in weight from 3 to 6 months, followed by a decrease from 6 to 12 months. Although these differences in SAMP8 do not reach statistical significance ($p = 0{,}08$ for the factor weight in SAMP8), the decrease in their body weight at 12 months old is likely due to their accelerated senescence, as loss of body weight is associated with the aging process itself [30], resulting in worsening and weakening.

Evolution of hippocampal PAS granules

Ageing in mice leads to the appearance and accumulation in the hippocampus of specific age-related polyglucosan aggregates, known as PAS granules, with an earlier increase observed in senescence-accelerated SAMP8 animals than in control ICR-CD1 mice, with non-accelerated senescence. In order to verify these events in the animals used in the present work, we quantified the number of hippocampal PAS granules for each animal (Fig. 6B). The statistical analysis performed by ANOVA, defining the variables strain and age at sacrifice as independent variables, indicated that both variables and their interaction have a significant effect on the number of PAS granules ($p < 0.01$ in all cases). Post-hoc comparisons indicate that SAMP8 animals had an increased amount of PAS granules respect to ICR-CD1 animals and that the amount of PAS granules increased with the ageing of the animals. The significant interaction indicates that, as expected according to the literature [13], ageing influences the two strains differently and markedly in SAMP8 animals. Specifically, 12-month-old SAMP8 mice showed more hippocampal granules than younger SAMP8 mice and, at this older stage, SAMP8 mice exhibited more hippocampal PAS granules than age-matched ICR-CD1 mice. As commented, SAMP8 animals begin to worsen and weaken before 12 months of age, which is reflected in both the decrease of their body weight and the marked increase of PAS granules in their hippocampus.

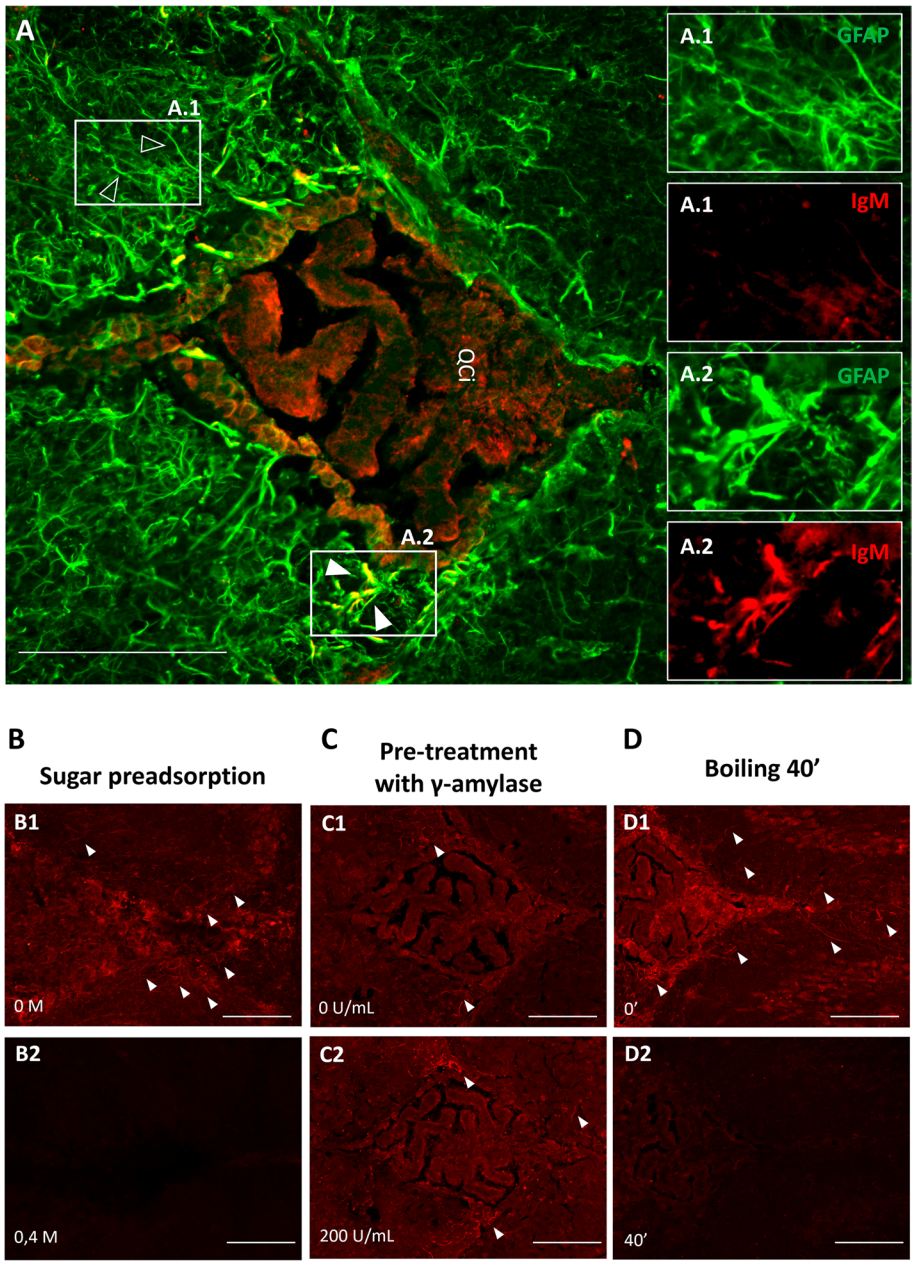

Fig. 5 Presence of IgM$^+$ astrocytes. **A** Representative section of zone 2 from a 12-month-old SAMP8 mouse immunostained with anti-GFAP (green), and IgM (red) antibodies (A); note that astrocytes not close to the fissures were IgM$^-$ (green-stained, empty arrowheads, A.1) while only the astrocytes closest to the fissures were IgM$^+$ (yellow (green + red)-stained, full arrowheads, A.2). **B** Effect of the preadsorption of IgM antibodies with a 0.4 M sugar mixture in IgM$^+$ astrocytes in a representative section of a 12-month-old SAMP8 mouse. **C** Effect of the pre-treatment with 200 U/mL of γ-amylase on the staining with IgM in IgM$^+$ astrocytes in a representative section of a 12-month-old SAMP8 mouse. **D** Effect of a 40 min boiling pre-treatment on the staining with IgM in IgM$^+$ astrocytes in a representative section of a 12-month-old SAMP8 mouse. Scale bars: 100 µm

Evolution of the amount of IgM$^+$ astrocytes

We quantified the IgM$^+$ astrocytes associated with the fissures. Figure 6C shows the amount of IgM$^+$ astrocytes across strains and ages. The statistical analysis performed by ANOVA, defining the variables strain and age at sacrifice as independent variables, indicated that the variable age has a significant effect ($p < 0{,}01$) on the presence of IgM$^+$ astrocytes as well as the interaction between both variables ($p < 0{,}05$), which indicates that the number of IgM$^+$ astrocytes increased with age differently in ICR-CD1 animals than in SAMP8 animals. Notably, 12-month-old SAMP8 mice displayed a higher number of

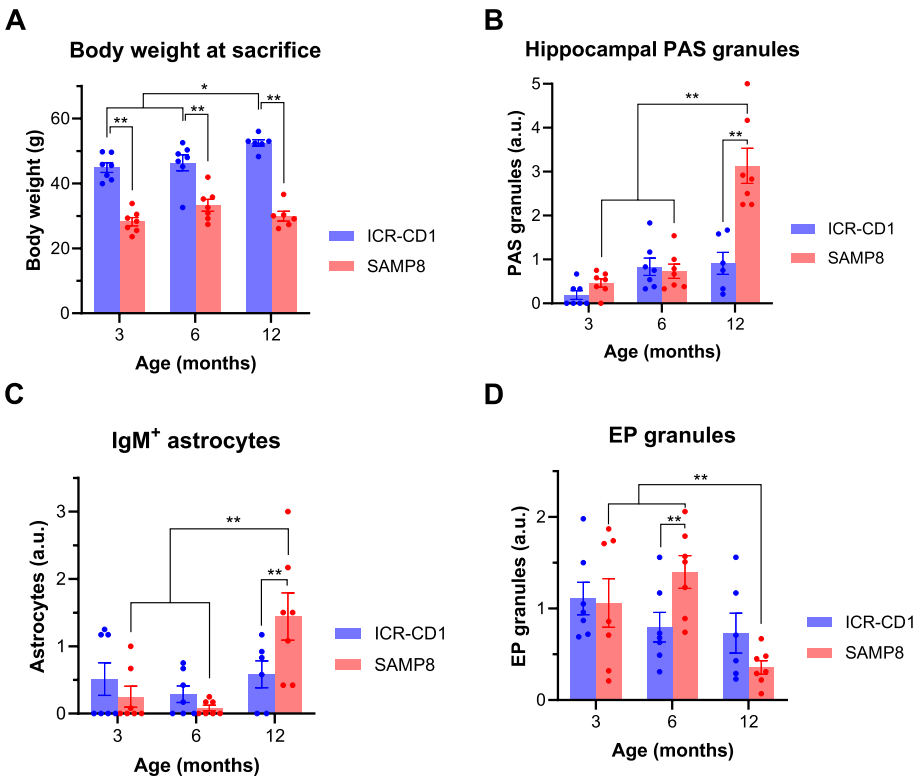

Fig. 6 **A** Body weight of ICR-CD1 and SAMP8 mice at the age of sacrifice. Data are shown as mean ± s.e.m. including individual values. **B-D** Scores obtained in ICR-CD1 and SAMP8 mice throughout the study regarding the amount of the hippocampal PAS granules (**B**), the amount of IgM$^+$ astrocytes in the vicinity of the fissures (**C**) and the amount of EP granules in the fissures (**D**). Bars show means ± s.e.m. of the scores from each experimental group, and the specific scores for each animal are also shown. *$p < 0.05$; ** $p < 0.01$. a.u.: arbitrary units

astrocytes reactive to IgM compared to younger SAMP8 mice. Furthermore, at this advanced age, SAMP8 mice presented more IgM$^+$ astrocytes than age-matched ICR-CD1 mice. These results were highly congruent with both the body weight evolution and the evolution of the amount of PAS granules, all reflecting the accelerated senescence in 12-month-old SAMP8 mice.

Evolution of the amount of EP granules

From each animal, we quantified the amount of EP granules in each region of interest of one coronal brain section, and we obtained the mean of the EP granules contained in the different regions, hence defining the score of EP granules for every animal. Then, using the score of EP granules from each animal, we studied the effects of age and strain in the amount of EP granules. Figure 6D shows the EP score per animal and the mean for each experimental group. The statistical analysis performed by ANOVA, defining the variables strain and age as independent variables, showed that age significantly affected EP granule score ($p < 0.01$) and that the interaction was also significant ($p < 0.05$), indicating that the effect of age on ICR-CD1 and SAMP8 strains differs. Post hoc comparisons indicate that 12-month-old SAMP8 mice show a significant decrease in these granules compared to 3- and 6-month-old animals, reflecting again the accelerated senescence in 12-month-old SAMP8 mice.

Integrative view or the results

Having observed how age and strain variables influenced the amount of PAS granules in the hippocampus, along with IgM$^+$ astrocytes and EP granules, we analysed the correlations among these variables. While there was a negative correlation between EP granules and both PAS granules and IgM$^+$ astrocytes ($\rho = -0.533$, $p < 0.01$, and $\rho = -0.605$, $p < 0.01$ respectively), PAS granules and IgM$^+$ astrocytes showed a positive correlation between them ($\rho = 0.787$, $p < 0.01$). Taken all together, this indicates that the age-related increase in PAS granules in the hippocampus, which is more pronounced in SAMP8 than in ICR-CD1 animals, is accompanied by an increase in IgM$^+$ astrocytes and a decline in EP granules in the fissures.

Discussion

The presence of neoepitopes in PAS granules from the mouse brain suggested the presence of neoepitopes in other brain structures, and this has been investigated in the present work. To this end, we examined structures reactive to natural IgM antibodies and discovered a kind of granules that differ from PAS granules but are also IgM-reactive. These granules, which have been named here EP granules because they are extraparenchymal (EP), are located in the deeper part of the longitudinal fissure, in the quadrigeminal cistern and also in the space we named the fissura magna, situated rostrally between the telencephalon and the diencephalon and caudally between the telencephalon and the mesencephalon.

This last space, the fissura magna, needs special attention. This region extends from the pineal gland and the central sulcus towards the roof of the third ventricle and then, in close contact with the interventricular foramina, connects the perimesencephalic cisterns: quadrigeminal, ambient, and interpeduncular cisterns [31]. Indeed, the dorsal structure of this area has been already described [32] as the connection of the subarachnoidal space (SAS) from the retrosplenial cortex and superior colliculus to the region adjacent to the lateral ventricles (Figs. 7A and B). This space connects the perimesencephalic cisterns and ensures CSF continuity across various brain cisterns, including the cisterna magna, while lying in proximity to the ventricular system and the choroid plexus [32]. Our findings about the distribution of EP granules and the observations of tracer distribution post-injection into the cisterna magna [33, 34], indicate a continuous space that connects the roof of the third ventricle to the interpeduncular cistern (Fig. 7C1). Notably, several works relating to this area refer to this space as a perivascular space [34] or use some correct but less practical expressions such as “a deep cleft linking the quadrigeminal, ambient and interpeduncular cisterns” [33]. In the absence of a defined nomenclature for this space in murine anatomy, we introduced the term "fissura magna" as the largest fissure within the mouse brain, mirroring the term used for the cisterna magna, the largest cistern in rodent brains. Analogous to the longitudinal or interhemispheric fissure that separates the two cortex hemispheres, or the transversal fissure which delineates the cerebellum from the cerebrum, the fissura magna distinctly separates the telencephalon from both the diencephalon and the

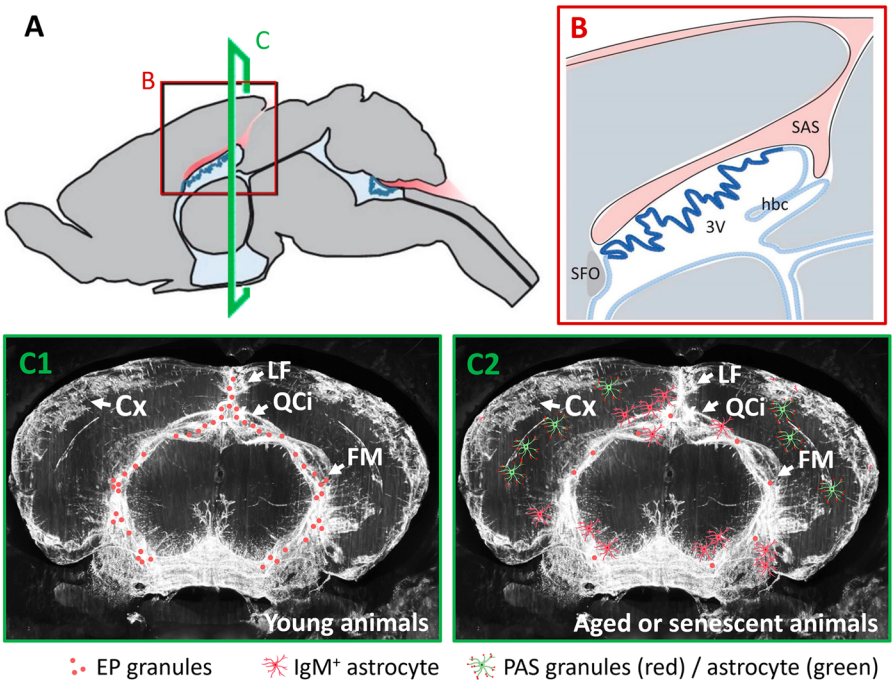

Fig. 7 **A** Drawing of a mouse brain from a sagital view highlighting the subarachnoidal space (SAS) in red and the choroid plexus in blue. **B** Magnified view from the window in A where the SAS (red) can be seen infiltrating the brain above the third ventricle (3 V) and the choroid plexus (blue). **C** C1 and C2 include a coronal view (corresponding to the region C of the image A) of a mouse brain with a fluorescent tracer injected in the cisterna magna. The tracer (white) is distributed along the longitudinal fissure, the quadrigeminal cistern and the fissura magna. Over this image, we include the pattern of EP granules, reactive IgM.$^{+}$ astrocytes and PAS granules in young (C1) and senescent (C2) animals. Cortex (Cx), fissura magna (FM), habenular commissure (hbc), longitudinal fissure (LF), quadrigeminal cistern (QCi), subfornical organ (SFO). A and B are adapted from [32]; C1 and C2 are adapted from [34]

mesencephalon. This space has also been noted in rat brains [35, 36], and we also suggest to apply the term fissura magna to describe them, as well as to use this nomenclature for the corresponding fissure in the brain of other mammals.

As previously mentioned, the injection of fluorescent tracers into the cisterna magna reveals a posterior staining in the space that corresponds to the fissura magna. Such observations, alongside with those of various paravascular spaces [37] and fissures like the hippocampal fissure that originate from the ambient cistern of the fissura magna, highlight the complex anatomy of the brain's CSF system. This system not only provides a protective cushion but also plays a pivotal role in immune surveillance and waste elimination [38–42]. On the other hand, the meninges are not only a physical barrier that protects the brain but also create a crucial space for immune surveillance. Meninges and CSF play a role in the clearance of metabolic waste from the brain through different pathways, which is essential for maintaining brain health and preventing neurological diseases [37, 42]. Indeed, antigens present in the CSF accumulate around the dural sinuses, where they are captured by antigen-presenting cells, which later present these antigens to patrolling T cells, facilitating a targeted immune response [43]. In this sense, we found that the EP granules are not associated with astrocytes, but with the fibroblasts contained in these regions. Fibroblasts have been documented in the brain parenchyma, in the perivascular spaces of the blood vessels, in the choroid plexus and in the pia mater. However, the role of these fibroblasts in healthy adults is just beginning to be studied [27]. Despite this lack of information, some researchers proposed that fibroblasts covering vessels facilitate fluid exchange between the CSF and perivascular spaces, thus linking the fibroblasts with the glymphatic system [44, 45]. Moreover, it is likely that there is signalling crosstalk between meningeal fibroblasts and neighbouring immune cells, and it has been proposed that fibroblasts are important elements linking the brain and the immune system [27]. In this regard, it seems coherent that fibroblasts may contain neoepitopes, which are targets of natural IgM antibodies but could also be presented to patrolling T cells.

Another finding of the present work is that some astrocytes placed in the glia limitans are also IgM^+. Interestingly, while EP granules are more prevalent in younger ages, the number of IgM^+ astrocytes and PAS granules increases with age (Figs. 7C1 and 7C2). This observation suggests a shift in how material is cleared from the brain, possibly due to a decreased production of CSF with age [46] or a decrease in the cleaning of the brain by the glymphatic system [47] which could both affect the ability of the brain to release material into the CSF. Thus, with age, these epitopes may tend to accumulate in the PAS granules and IgM^+ astrocytes. Provided that IgM^+ astrocytes are present in the glia limitans, in the boundaries of the brain to the CSF, these cells might be accumulating this material with advancing ages, suggesting a deficiency in clearance mechanisms with ageing and an alteration in the brain immune surveillance. In addition, this is supported by the fact that, in an age-dependent manner, bordering astrocytes in humans brain can also accumulate waste substances associated with neoepitopes [40]. Contrarily, young animals contain a high content of EP granules. Thus, the presence of these IgM^+ granular structures could be seen as part of the cleaning mechanism against the accumulation of potentially harmful aggregates, or could be related to the physiological brain-CSF immune surveillance, where brain abnormal structures are transferred to the fibroblasts or released into the CSF, following glymphatic flow [45]. These EP granules, despite being immunologically active, do not seem to induce any inflammatory reaction, indicating that the immune surveillance in this pathway does not trigger brain inflammatory responses.

As shown here, EP granules contain neoepitopes, as both PAS granules and human wasteosomes do [21, 48]. The inhibition of IgM binding to EP granules when IgMs were preabsorbed with a mixture of sugars, as also happened to PAS granules or wasteosomes [23, 49], suggests that the epitopes recognized by the IgMs have also a carbohydrate nature, highlighting a potential commonality in their immunological recognition. However, EP granules exhibit several differences respect to the PAS granules, such as the absence of astrocytic association, absence of reactivity for both α-p62 and α-GS, absence of PAS staining and low susceptibility to amylase digestion, all of them characteristics of PAS granules [18, 20, 39, 50].

The differential PAS staining and response to amylase points the presence of different polyglucosan content. The PAS staining is used to detect complex polysaccharides in tissues [51]. This method relies on the oxidizing action of periodic acid, which converts the free hydroxyl groups in these molecules into dialdehydes. These dialdehydes then react with Schiff's reagent, resulting in a magenta-pink complex. Hence, PAS granules contain a significant amount of polyglucosan structures, whereas EP granules are likely to possess a small amount of them, or alternatively the polyglucosans must have a different composition, less sensitive to amylase digestion and PAS staining.

All these observations and differences seem to indicate a different process involved in these structures. While PAS granules are structures originated in astrocytes and may have a protective function retaining unwanted or harmful materials, and IgM^+ astrocytes could also

be related to the accumulation of harmful materials, EP granules are related to fibroblasts and seem to be part of a physiological function in brain cleansing or brain-CSF immune surveillance.

Conclusions

Finally, and to conclude, the present work reports the discovery of two brain-related structures that contain neo-epitopes of carbohydrate nature. On one side, the EP granules, which are related to fibroblasts, are present mainly in young animals, and may be part of the brain cleansing mechanism or brain-CSF immune surveillance. On the other part, some astrocytes that are IgM^+ and which, as happened with PAS granules, are present mainly in aged or senescent animals, may have a protective function retaining and isolating unwanted or harmful materials. Moreover, the specific localisation of these EP granules and IgM^+ astrocytes points out the importance of the fissura magna, situated between the telencephalon and both the diencephalon and the mesencephalon, in these brain-related cleaning and immune functions.

Supplementary Information

The online version contains supplementary material available at https://doi.org/10.1186/s12979-024-00460-1.

Supplementary Material 1: Supplementary figure 1: A-F: Effect of the preadsorption of IgM antibodies with increasing concentrations of a sugar mixture in the IgM staining (red) of EP granules from the fissures (zone 2, A, B and C) and in PAS granules from the hippocampus (D, E and F). G-L: Effect of the pre-treatment with increasing concentrations of γ-amylase on the staining with IgM in EP granules (zone 2, G, H and I) and in PAS granules from the hippocampus (J, K and L)

Supplementary Material 2: Supplementary figure 2: Quantification in arbitrary units (a.u.) of EP granules across strains (ICR-CD1 & SAMP8), ages and regions of the fissura magna. X-axis regions correspond to the 1-8 numbered regions described. Values for regions 3-8 are averaged between left and right hemispheres. Data are expressed as mean ± s.e.m.

Acknowledgements

C.R. and R.A received pre-doctoral fellowships from the Formación de Personal Investigador (FPI2022, C.R) and from Formación de Profesorado Universitario (FPU2022, R.A), both from the Spanish Ministerio de Ciencia, Innovación y Universidades. MR received the postdoctoral fellowship Margarita Salas funded by the Spanish Ministry of Universities with NextGenerationEU funds.

Authors' contributions

Conception and Design: CR, MR, JV, CP, JdV. Acquisition of Data: CR, MR, RA, MS, JV, CP, JdV. Statistical Analysis: JV, JdV. Execution: CR, MR, RA, MS, JV, CP, JdV. Interpretation of data: CR, JV, CP, JdV. Fissura magna concept ideation: JV. Writing and revising: CR, JV, CP, JdV. Critical review for important intellectual content: all authors. All authors have approved the final version of the manuscript.

Funding

This article is part of the project PID2023-148768OA-I00 and PID2020-115475 GB-I00, both funded by MCIN/ AEI/https://doi.org/10.13039/501100011033, and Ajuts del Vicerectorat de recerca de la UB. We thank the Generalitat de Catalunya for funding our research group (2021/SGR00288).

Availability of data and materials

The datasets used and/or analysed during the current study are available from the corresponding author on reasonable request.

Declarations

Ethics approval and consent to participate

Studies were performed in accordance with the institutional guidelines for the care and use of laboratory animals established by the Ethical Committee for Animal Experimentation at the University of Barcelona under the regulations of the European Directive 2010/63/UE and the Spanish RD 53/2013.

Consent for publication

Not applicable.

Competing interests

The authors declare that they have no competing interests.

Author details

[1]Secció de Fisiologia, Departament de Bioquímica i Fisiologia, Facultat de Farmàcia i Ciències de L'Alimentació, Universitat de Barcelona, Barcelona 08028, Spain. [2]Institut de Neurociències, Universitat de Barcelona, Barcelona 08035, Spain. [3]Centros de Biomedicina en Red de Enfermedades Neurodegenerativas (CIBERNED), Madrid 28031, Spain.

Received: 4 June 2024 Accepted: 13 August 2024
Published online: 21 August 2024

References

1. Hou Y, Dan X, Babbar M, Wei Y, Hasselbalch SG, Croteau DL, et al. Ageing as a risk factor for neurodegenerative disease. Nat Rev Neurol. 2019;15:565–81. https://doi.org/10.1038/s41582-019-0244-7.
2. Lin CW, Chang LC, Ma T, Oh H, French B, Puralewski R, et al. Older molecular brain age in severe mental illness. Mol Psychiatry. 2021;26:3646–56. https://doi.org/10.1038/s41380-020-0834-1.
3. Yeoman M, Scutt G, Faragher R. Insights into CNS ageing from animal models of senescence. Nat Rev Neurosci. 2012;13:435–45. https://doi.org/10.1038/nrn3230.
4. Wyss-Coray T. Ageing, neurodegeneration and brain rejuvenation. Nature. 2016;539:180–6. https://doi.org/10.1038/nature20411.
5. Peters R. Ageing and the brain. Postgrad Med J. 2006;82:84–8. https://doi.org/10.1136/pgmj.2005.036665.
6. Ikeda K, Sugiura Y, Nakao H, Nakano M. Thermodynamics of oligomerization and Helix-to-sheet structural transition of amyloid β-protein on anionic phospholipid vesicles. Biophys Chem. 2024;310: 107248. https://doi.org/10.1016/j.bpc.2024.107248.
7. Paterno G, Bell BM, Gorion KMM, Prokop S, Giasson BI. Reassessment of Neuronal Tau Distribution in Adult Human Brain and Implications for Tau Pathobiology. Acta Neuropathol Commun. 2022;10:94. https://doi.org/10.1186/s40478-022-01394-9.
8. Riba M, del Valle J, Romera C, Alsina R, Molina-Porcel L, Pelegrí C, et al. Uncovering tau in wasteosomes (corpora amylacea) of Alzheimer's disease patients. Front Aging Neurosci. 2023;15:1110425. https://doi.org/10.3389/fnagi.2023.1110425.
9. Uemura MT, Suh ER, Robinson JL, Brunden KR, Grossman M, Irwin DJ, et al. Abundant copathologies of polyglucosan bodies, frontotemporal lobar degeneration with TDP-43 inclusions and ageing-related tau astrogliopathy in a family with a GBE1 mutation. Neuropathol Appl Neurobiol. 2023;49: e12865. https://doi.org/10.1111/nan.12865.
10. Jucker M, Walker LC, Kuo H, Tian M, Ingram DK. Age-related fibrillar deposits in brains of C57BL/6 mice - A review of localization, staining characteristics, and strain specificity. Mol Neurobiol. 1994;9:125–33. https://doi.org/10.1007/BF02816112.
11. Lamar CH, Hinsman EJ, Henrikson CK. Alterations in the hippocampus of aged mice. Acta Neuropathol. 1976;36:387–91. https://doi.org/10.1007/BF00699644.

12. Soontornniyomkij V, Risbrough VB, Young JW, Soontornniyomkij B, Jeste DV, Achim CL. Increased hippocampal accumulation of autophagosomes predicts short-term recognition memory impairment in aged mice. Age (Dordr). 2012;34:305–16. https://doi.org/10.1007/s11357-011-9234-4.
13. del Valle J, Duran-Vilaregut J, Manich G, Casadesús G, Smith MAMA, Camins A, et al. Early amyloid accumulation in the hippocampus of SAMP8 mice. J Alzheimer's Dis. 2010;19:1303–15. https://doi.org/10.3233/JAD-2010-1321.
14. del Valle J, Duran-Vilaregut J, Manich G, Pallàs M, Camins A, Vilaplana J, et al. Cerebral amyloid angiopathy, blood-brain barrier disruption and amyloid accumulation in SAMP8 mice. Neurodegener Dis. 2011;8:421–9. https://doi.org/10.1159/000324757.
15. Mitsuno S, Takahashi M, Gondo T, Hoshii Y, Hanai N, Ishihara T, et al. Immunohistochemical, conventional and immunoelectron microscopical characteristics of periodic acid-Schiff-positive granules in the mouse brain. Acta Neuropathol. 1999;98:31–8. https://doi.org/10.1007/s00401051048.
16. Akiyama H, Kameyama M, Akiguchi I, Sugiyama H, Kawamata T, Fukuyama H, et al. Periodic acid-Schiff (PAS)-positive, granular structures increase in the brain of senescence accelerated mouse (SAM). Acta Neuropathol. 1986;72:124–9. https://doi.org/10.1007/BF00685973.
17. Kuo H, Ingram DK, Walker LC, Tian M, Hengemihle JM, Jucker M. Similarities in the age-related hippocampal deposition of periodic acid-Schiff-positive granules in the senescence-accelerated mouse (SAM P8) and C57BL/6 mouse strains. Neuroscience. 1996;74:733–40. https://doi.org/10.1016/0306-4522(96)00169-8.
18. Manich G, Cabezón I, Augé E, Pelegrí C, Vilaplana J. Periodic acid-Schiff granules in the brain of aged mice: From amyloid aggregates to degenerative structures containing neo-epitopes. Ageing Res Rev. 2016;27:42–55. https://doi.org/10.1016/j.arr.2016.03.001.
19. Manich G, Cabezón I, Camins A, Pallàs M, Liberski PP, Vilaplana J, et al. Clustered granules present in the hippocampus of aged mice result from a degenerative process affecting astrocytes and their surrounding neuropil. Age (Omaha). 2014;36:9690. https://doi.org/10.1007/s11357-014-9690-8.
20. Augé E, Pelegrí C, Manich G, Cabezón I, Guinovart JJ, Duran J, et al. Astrocytes and neurons produce distinct types of polyglucosan bodies in Lafora disease. Glia. 2018;66:2094–107. https://doi.org/10.1002/glia.23463.
21. Manich G, Augé E, Cabezón I, Pallàs M, Vilaplana J, Pelegrí C. Neo-epitopes emerging in the degenerative hippocampal granules of aged mice can be recognized by natural IgM auto-antibodies. Immun Ageing. 2015;12:1–7. https://doi.org/10.1186/s12979-015-0050-z.
22. Augé E, Duran J, Guinovart JJ, Pelegrí C, Vilaplana J. Exploring the elusive composition of corpora amylacea of human brain. Sci Rep. 2018;8:13525. https://doi.org/10.1038/s41598-018-31766-y.
23. Manich G, del Valle J, Cabezón I, Camins A, Pallàs M, Pelegrí C, et al. Presence of a neo-epitope and absence of amyloid beta and tau protein in degenerative hippocampal granules of aged mice. Age (Omaha). 2014;36:151–65. https://doi.org/10.1007/s11357-013-9560-9.
24. Paxinos G, Franklin KBJ. Paxinos and franklin's the mouse brain in stereotaxic coordinates. Academic press: Acad. Press; 2019.
25. It's time to talk about ditching statistical significance. Nature. Nature Publishing Group; 2019. p. 283. https://doi.org/10.1038/d41586-019-00874-8
26. Allen Institute for Brain Science. Allen Mouse Brain Atlas . Allen Mouse Brain Atlas. 2004. Available from: https://connectivity.brain-map.org/static/referencedata/experiment/siv/100140665?imageId=102117898&imageType=NISSL&initImage=NISSL&filter=contrast&filterVals=0.5,0.5&x=4984&y=4032&z=5
27. Dorrier CE, Jones HE, Pintarić L, Siegenthaler JA, Daneman R. Emerging roles for CNS fibroblasts in health, injury and disease. Nat Rev Neurosci. 2022;23:23–34. https://doi.org/10.1038/s41583-021-00525-w.
28. Takeda T, Hosokawa M, Takeshita S, Irino M, Higuchi K, Matsushita T, et al. A new murine model of accelerated senescence. Mech Ageing Dev. 1981;17:183–94. https://doi.org/10.1016/0047-6374(81)90084-1.
29. Kimura K, Takeuchi K. Aging and longevity of the Jel: ICR Mouse. Okajimas Folia Anat Jpn. 1988;65:35–42. https://doi.org/10.2535/ofaj1936.65.1_35.
30. Bales CW, Ritchie CS. Sarcopenia, weight loss, and nutritional frailty in the elderly. Annu Rev Nutr. 2002;22:309–23. https://doi.org/10.1146/annurev.nutr.22.010402.102715.
31. Mani RL, Newton TH, Glickman MG. The superior cerebellar artery: an anatomic-roentgenographic correlation. Radiology. 1968;91:1102–8. https://doi.org/10.1148/91.6.1102.
32. Greiner T, Manzhula K, Baumann L, Kaddatz H, Runge J, Keiler J, et al. Morphology of the murine choroid plexus: Attachment regions and spatial relation to the subarachnoid space. Front Neuroanat. 2022;16:1–12. https://doi.org/10.3389/fnana.2022.1046017.
33. Bedussi B, Van Der Wel NN, de Vos J, Van Veen H, Siebes M, VanBavel E, et al. Paravascular channels, cisterns, and the subarachnoid space in the rat brain: A single compartment with preferential pathways. J Cereb Blood Flow Metab. 2017;37:1374–85. https://doi.org/10.1177/0271678X16655550.
34. Jacob L, de Brito Neto J, Lenck S, Corcy C, Benbelkacem F, Geraldo LH, et al. Conserved meningeal lymphatic drainage circuits in mice and humans. J Exp Med. 2022;219. https://doi.org/10.1084/jem.20220035
35. Magdoom KN, Brown A, Rey J, Mareci TH, King MA, Sarntinoranont M. MRI of Whole Rat Brain Perivascular Network Reveals Role for Ventricles in Brain Waste Clearance. Sci Rep. 2019;9:11480. https://doi.org/10.1038/s41598-019-44938-1.
36. Gómez-De Frutos MC, García-Suárez I, Laso-García F, Diekhorst L, Otero-Ortega L, Alonso-López E, et al. Identification of brain structures and blood vessels by conventional ultrasound in rats. J Neurosci Methods [Internet]. 2020;346: 108935. https://doi.org/10.1016/j.jneumeth.2020.108935.
37. Coles JA, Myburgh E, Brewer JM, McMenamin PG. Where are we? The anatomy of the murine cortical meninges revisited for intravital imaging, immunology, and clearance of waste from the brain. Prog Neurobiol. 2017;156:107–48. https://doi.org/10.1016/j.pneurobio.2017.05.002.
38. Iliff JJ, Wang M, Liao Y, Plogg BA, Peng W, Gundersen GA, et al. A paravascular pathway facilitates CSF flow through the brain parenchyma and the clearance of interstitial solutes, including amyloid β. Sci Transl Med. 2012;4:147ra11. https://doi.org/10.1126/scitranslmed.3003748
39. Riba M, Campo-Sabariz J, Tena I, Molina-Porcel L, Ximelis T, Calvo M, et al. Wasteosomes (corpora amylacea) of human brain can be phagocytosed and digested by macrophages. Cell Biosci. 2022;12:1–17. https://doi.org/10.1186/s13578-022-00915-2.
40. Riba M, Augé E, Campo-Sabariz J, Moral-Anter D, Molina-Porcel L, Ximelis T, et al. Corpora amylacea act as containers that remove waste products from the brain. Proc Natl Acad Sci U S A. 2019;116:26038–48. https://doi.org/10.1073/2Fpnas.1913741116.
41. Riba M, Romera C, Alsina R, Alsina-Scheer G, Pelegrí C, Vilaplana J, et al. Analyzing the Virchow pioneering report on brain corpora amylacea: shedding light on recurrent controversies. Brain Struct Funct. 2023;228:1371–8. https://doi.org/10.1007/s00429-023-02664-5.
42. Yamada S, Ito H, Tanikawa M, Ii S, Otani T, Wada S, et al. Age-related changes in cerebrospinal fluid dynamics in the pathogenesis of chronic hydrocephalus in adults. World Neurosurg. 2023;178:351–8. https://doi.org/10.1016/j.wneu.2023.07.110.
43. Rustenhoven J, Drieu A, Mamuladze T, de Lima KA, Dykstra T, Wall M, et al. Functional characterization of the dural sinuses as a neuroimmune interface. Cell. 2021;184:1000-1016.e27. https://doi.org/10.1016/j.cell.2020.12.040.
44. Mastorakos P, McGavern D. The anatomy and immunology of vasculature in the central nervous system. Sci Immunol. 2019;4:492. https://doi.org/10.1126/sciimmunol.aav0492.
45. Rasmussen MK, Mestre H, Nedergaard M. Fluid transport in the brain. Physiol Rev. 2022;102:1025–151. https://doi.org/10.1152/physrev.00031.2020.
46. May C, Kaye JA, Atack JR, Schapiro MB, Friedland RP, Rapoport SI. Cerebrospinal fluid production is reduced in healthy aging. Neurology. 1990;40:500. https://doi.org/10.1212/wnl.40.3_part_1.500.
47. Riba M, del Valle J, Molina-Porcel L, Pelegrí C, Vilaplana J. Wasteosomes (corpora amylacea) as a hallmark of chronic glymphatic insufficiency. Proc Natl Acad Sci U S A. 2022;119: e2211326119. https://doi.org/10.1073/pnas.2211326119.
48. Augé E, Bechmann I, Llor N, Vilaplana J, Krueger M, Pelegrí C. Corpora amylacea in human hippocampal brain tissue are intracellular bodies that exhibit a homogeneous distribution of neo-epitopes. Sci Rep. 2019;9:2063. https://doi.org/10.1038/2Fs41598-018-38010-7.
49. Riba M, Augé E, Tena I, del Valle J, Molina-Porcel L, Ximelis T, et al. Corpora Amylacea in the Human Brain Exhibit Neoepitopes of a Carbohydrate

Nature. Front Immunol. 2021;12:9–12. https://doi.org/10.3389/fimmu.2021.618193.
50. Riba M, del Valle J, Augé E, Vilaplana J, Pelegrí C. From corpora amylacea to wasteosomes: History and perspectives. Ageing Res Rev. 2021;72:101484. https://doi.org/10.1016/j.arr.2021.101484.
51. McManus JF, Cason JE. Carbohydrate histochemistry studied by acetylation techniques I. Periodic acid methods. J Exp Med. 1950;91:651–4. https://doi.org/10.1084/jem.91.6.651.

Publisher's Note